International Journal of Innovative
Computing, Information and Control
Volume **8**, Number **12**, December **2012**

 ISSN 1349-4198
pp. 8199–8214

SURROGATE NEURAL NETWORK AND MULTI-OBJECTIVE DIRECT ALGORITHM FOR THE OPTIMIZATION OF A SWISS-ROLL TYPE RECUPERATOR

Yau-Zen Chang[1], Kao-Ting Hung[1], Hsin-Yi Shih[1] and Zhi-Ren Tsai[2]

[1]Department of Mechanical Engineering
Chang Gung University
No. 259, Wen-Hwa 1st Road, Kwei-Shan, Tao-Yuan 33302, Taiwan
hyshih@mail.cgu.edu.tw

[2]Department of Computer Science and Information Engineering
Asia University
No. 500, Lioufeng Road, Wufeng, Taichung 41354, Taiwan
ren@asia.edu.tw

Received September 2011; revised March 2012

Abstract. *Micro-turbines are promising high power-density engines for distributed power generation. In this paper, an innovative optimization procedure is proposed to design a Swiss-roll type recuperator that recovers the exhaust heat of a micro gas turbine. There are several design parameters to be optimized for the recuperator, including the number of turns, channel width, plate thickness, and mass flow rate. The complex interconnections of the parameters make it difficult to analyze the process and select an adequate design with the highest effectiveness and lowest pressure drop. In order to reduce the number of numerical analysis required in the two-objective optimization process, a neural network was trained to serve as a surrogate model for the analysis and a multi-objective DIRECT (DIviding RECTangle) algorithm, named as MO-DIRECT, is proposed. After merely 5 iterations of MO-DIRECT search, we were able to find a min-max solution with prediction error lower than 4%. In the search process, only 24 numerical simulations are required to achieve the result with totally 2,313 steps conducted in the MO-DIRECT search, rather than 35,343 simulations for an exhaustive search.*
Keywords: Recuperator, Heat exchanger design, Multi-objective optimization

1. **Introduction.** Micro-turbines with output power in the range of 25-300 kW are promising high power-density engines for distributed power generation [1]. In the past few years, an even smaller micro-turbine with the power output in the range of 5-10 kW, known as the personal turbine (PT), has attracted much attention [2]. It is a compact, silent running combustion turbine to provide the total energy needs for an average home or small factory. However, for micro-turbines, it is difficult to achieve high efficiency without heat recuperation or heat regeneration, which recovers the heat from exhaust gases to improve the cycle efficiency, as well as to decrease the fuel requirement. A recuperator then becomes mandatory for micro-turbines [3]. Following this trend, an innovative micro gas turbine with a Swiss-roll type recuperator is proposed, and the proposed unit potentially has a compact size with higher efficiency [4-6]. Based on the feasibility study [4], the overall thermal efficiency increases with the increase of recuperator effectiveness, but it decreases with the rise of pressure loss. Therefore, thermal design of the Swiss-roll recuperator with high effectiveness and low-pressure loss is the key to the success of the proposed micro-turbine.

The Swiss-roll recuperator is composed of two flat plates wrapped around each other, creating two concentric channels of rectangular cross-section. It recovers part of the exhaust heat and preheats the incoming air, effectively raising overall efficiency. Although using flat plates suffers from small heat transfer coefficient, the arrangement has lower pressure loss and simpler model, as assumed in this preliminary study. The idea to use the Swiss-roll type recuperator came from the devices named heat-recirculating or excess enthalpy burners in 1975 [7,8]. Recently, this technology has been reemerged for the studies of micro power generation using combustion [9]. The Swiss-roll type configuration is employed as heaters for thermoelectric power systems [10-13], and is proposed as one of the compact heat exchanges for a new generation of high temperature solar receivers [14].

The thermal design and performance characteristics of the Swiss-roll recuperator have been studied through the theoretical and modeling analysis in [5]. There are several design parameters for the Swiss-roll recuperator, including number of turns, channel width, plate thickness, and mass flow rate. Results of the analysis showed that both effectiveness and pressure drop of the Swiss-roll recuperator increase with the increase of the number of turns. Increasing channel width then decreases both effectiveness and pressure loss. Besides, thicker plate benefits the heat transfer rate, consequently the effectiveness, but deteriorates the pressure loss because of larger flow resistance. The flow velocity is higher for a smaller channel width at the same flow rate, which will enhance the convective heat transfer. As the mass flow rate increases, effectiveness decreases while pressure loss rises.

The complex interconnection of the design parameters makes it difficult to analyze the process and select adequate parameter values. It is also unpractical to assess the performance of every possible configuration through computationally intensive simulations. Optimization of the thermal system [15] is typical of many practical industrial design problems with multiple objects [16] that require extensive computation. In order to reduce the amount of computation in the optimization process, a neural network [17] is employed as surrogate model [18], and a multi-objective DIRECT algorithm, abbreviated as MO-DIRECT, is proposed. The algorithm is a modified multi-objective version of the DIRECT (DIviding RECTangle) algorithm [19], which is an effective single-objective global optimization scheme [20] with systematic and decisive search steps.

2. The System under Investigation – Swiss-Roll Recuperator.

As shown in Figure 1, the Swiss-roll type recuperator surrounds the combustor for the innovative micro gas turbine. The Swiss-roll recuperator is designed as a counter-flow spiral-plate heat exchanger, which is a typical distributed parameter system [21]. The hot fluid enters at the center of the recuperator unit and flows outward towards the periphery. On the contrary, the cold fluid enters from the periphery and flows towards the center. By wrapping up the heat exchanger in the shape of a Swiss roll, the dissipated heat can be effectively reduced. The heat transfer between the windings and the core combustor is actually an integral part of the thermal system. High overall heat transfer coefficients, high thermal effectiveness and small pressure loss are the advantages of this configuration.

As mentioned above, effectiveness and pressure loss of the recuperator are two important characteristics in the thermal design. For example, from the cycle analysis for the baseline designs (power output of 9.3 kW with airflow rate at 0.154 kg/sec; compression ratio being 2.8; the turbine inlet temperature being 900 °C and the rotor speed being 130000 rpm), a swiss-roll recuperator with effectiveness of 0.85 and pressure drop below 10% is required to achieve the state-of-art performance [4]. The question is then how to design the recuperator to meet these requirements. In this section, the design procedures are

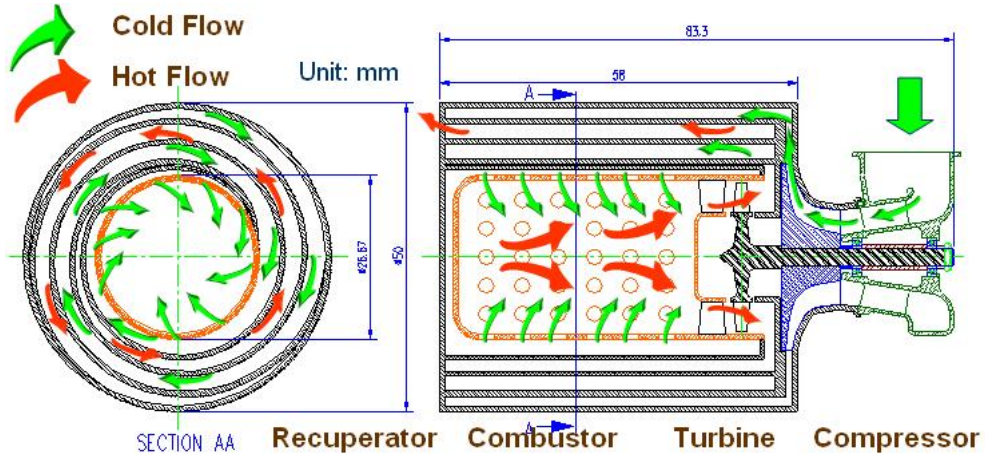

FIGURE 1. The micro gas turbine under study, showing a Swiss-roll recuperator surrounding the combustor

firstly through the thermal analysis to find basic configuration design parameters, and then construct the numerical model for performance analysis.

Notations used in the following investigation are listed as follows.

A	Area
c	Specific heat
ε	Effectiveness
F	Correction factor
$\dot{m}$	Mass flow rate
n	Number of turns
NTU	Number of transfer units (NTU)
ΔP	Pressure loss
q	Heat transfer rate
r_i	Core radius
Δr	Channel width
R	Ratio of the heat capacity between cold and hot flows
ΔT_m	Log mean temperature difference (LMTD)
T	Temperature
U	Universal heat transfer coefficient

2.1. **Thermal analysis.** For a counter-flow heat exchanger shown in Figure 1, the heat transfer between hot and cold flows can be expressed as:

$$q = \dot{m}_c c_c (T_{c1} - T_{c2}) = \dot{m}_h c_h (T_{h1} - T_{h2}) = UAF\Delta T_m \tag{1}$$

where U is the universal heat transfer coefficient, F is the correction factor and ΔT_m is the log mean temperature difference. The subscripts c and h represent the cold and hot channels, respectively. The effectiveness of the heat exchanger ε is defined as the ratio of the actual heat transfer over the maximum possible heat transfer ($q_{\max} = (\dot{m}c)_{\min}(T_{h1} - T_{c2})$), and is expressed as:

$$\varepsilon = \frac{q}{q_{\max}} = \frac{\dot{m}c_c(T_{c1} - T_{c2})}{(\dot{m}c)_{\min}(T_{h1} - T_{c2})} \text{ or } \frac{\dot{m}c_h(T_{h1} - T_{h2})}{(\dot{m}c_h)(T_{h1} - T_{c2})},$$

depending on which fluid, cold or hot, with smaller heat capacity. Here the heat capacity in cold flows is smaller, we have that $(\dot{m}c)_{\min} = \dot{m}_c c_c$, and

$$\varepsilon = \frac{T_{c1} - T_{c2}}{T_{h1} - T_{c2}}. \tag{2}$$

By introducing the number of transfer unit, $NTU \equiv \frac{UA}{(\dot{m}c)_{\min}}$, Equation (1) becomes the following relation:

$$F \times NTU = \varepsilon \frac{(T_{h1} - T_{c2})}{\Delta T_m}, \tag{3}$$

which is the major equation for the preliminary design of the Swiss-roll recuperator.

Since the Swiss-roll recuperator resembles the spiral-plate heat exchanger, the correction factor for counter-flow spiral-plate heat exchange is used [22,23]. If we define the ratio of the heat capacity between cold and hot flows as R, where $R = \dot{m}_c C_c / \dot{m}_h C_h$, the correction factor F for a spiral exchanger is simply a function of NTU per turn, i.e., NTU/n, as follows [23]:

If $R = 1$,

$$F \cong \frac{n}{NTU} \tanh\left(\frac{NTU}{n}\right) \tag{4}$$

If $R \neq 1$,

$$F \cong \frac{1}{(1-R)NTU/n} \ln\left(1 + \frac{1-R}{1/\varepsilon_i - 1}\right) \tag{5}$$

where

$$\varepsilon_i = \frac{1 - \exp\left[-(1+R)NTU/n\right]}{1+R} \tag{6}$$

For a desired effectiveness ε with given inlet temperature of hot and cold flows (T_{h1}, T_{c2}), pairs of (n, NTU) can be found from Equation (3). Once the number of turns n and the number of heat transfer unit NTU are determined, the width of the channels can be derived using a new analytical approximation for F as [24]:

$$F = z \ln\left(1 + \frac{1}{z+x}\right) \tag{7}$$

where

$$x = y^2/(1+2y) \tag{8}$$

$$y = r_i/(2n\Delta r) \tag{9}$$

$$z = (1+2y)/[(NTU/n)^2 R] \tag{10}$$

The parameter y is the core radius r_i divided by the total width of the double spiral pack of $2n$ channels, with the individual channel width being Δr. Therefore, for the Swiss-roll recuperator to achieve certain effectiveness, the number of turns, corresponding number of transfer unit, and the channel width can be estimated with this thermal design method.

2.2. **Model analysis.** A numerical model was carried out for fluid dynamics and heat transfer analysis of the configuration. Both two-dimensional and three-dimensional configurations were constructed to represent two limiting scenarios. The two-dimensional model computes the ideal case with adiabatic boundary conditions, and the three-dimensional model is for the case with heat loss from both sides while the ambient temperature is 300 K on the boundary. The fluid at the inlet of the cold channel is compressed air from the compressor, and the hot gas at the inlet of the hot channel is combusted gas through the turbines. The outlet boundary conditions are gradient-free. For the simplicity of the model, air is used as the fluid media for both channels.

The resultant Navier-Stokes equations of the steady and compressible $k-\varepsilon$ turbulent flows with heat transfer are solved with STAR-CD, a well-known Computational Fluid Dynamics software [25], using the SIMPLE algorithm [26]. Totally 19,952 grids and 602,640

grids are used for two-dimensional and three-dimensional calculations, respectively. The grid independence has been checked.

The simulation results from the two-dimensional model are demonstrated in Figure 2, where the temperature and pressure distributions are presented for the Swiss-roll recuperator with basic design parameters, that is, 6-turns recuperator with cold channel width of 5.8 mm separated by 1.4 mm-thick plates, where hot channel width is kept 1.5 times of cold channel width. The mass flow rate is 0.154 kg/s, and the core radius of the can combustor is assumed to be 25 mm.

These results indicate that, in hot channel, the inlet temperature of hot gas is 1,016 K, and it is cooled to 673.4 K at the outlet. On the other hand, temperature of cold air is heated from 411 K to 759.3 K in cold channel. The effectiveness of the recuperator is estimated as 0.60. The pressure distribution, in terms of the relative value to the inlet pressure, shows that the inlet pressure for the exhaust gas is 1.12 atm (113.5 kPa) in

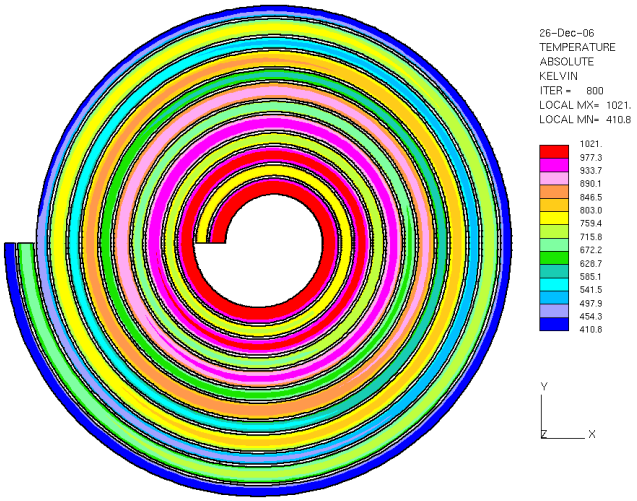

(a) The temperature distribution

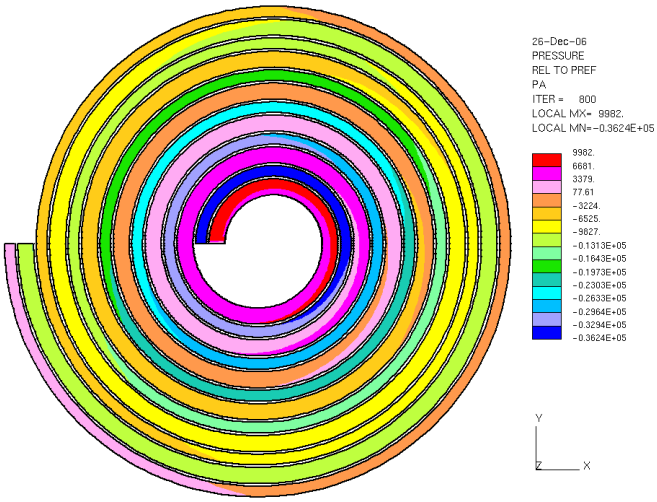

(b) The pressure distribution

FIGURE 2. Simulated characteristics of a 6-turns Swiss-roll recuperator under baseline design

the hot channel, and a decrease of 12.3 kPa was found at the exit. The pressure loss is 10.8%. For cold channel, the inlet pressure of the compressed air is 2.77 atm (280.6 kPa), and a drop of 33.4 kPa was obtained, approximately 11.9% pressure loss through the recuperator.

The above analysis clearly demonstrates that the baseline design is not optimal when both the effectiveness and the pressure loss are considered simultaneously. In the following investigation, we choose four parameters for the Swiss-roll type recuperator design: the number of turns n, cold channel width Δr, plate thickness d, and mass flow rate $\dot{m}$. The design goal is to build a recuperator with the highest effectiveness P_1 and lowest pressure drop P_2. The scheme for multi-objective optimization is then proposed and presented next.

3. **The Proposed Scheme for Multi-objective Optimization.** We propose to apply a modified version of the DIRECT optimization algorithm [19,27] to optimize the Swiss-roll recuperator. The name of the DIRECT algorithm is an abbreviation of DIviding RECTangles, describing a specific manipulation procedure. Developed by Jones et al. in 1993, the procedure is an effective implementation of multidimensional Lipschitzian optimization without the Lipschitz constant [27]. It is deterministic, guaranteed to converge, and has a very fast convergence rate without trapping in local extremes [28-30].

The design variables in the DIRECT algorithm correspond to coordinates of a point in an n-dimensional search space, which can be viewed as an n-dimensional hyper-box. By employing the principle of "Divide and Conquer", the algorithm proceeds by partitioning this hyper-box into smaller hyper-boxes, each of which has its center evaluated for objective functions (cost functions), and select promising hyper-boxes for further division.

The selection of these hyper-boxes is based on both box size and objective function value at center points. According to [19,28], a potentially optimal hyper-box in a single objective minimization problem is defined as follows. Let x_i denote the coordinate vector of the center point of an arbitrary hyper-box i, and d_i the distance from its center point to its vertex, which is an index of box size. Besides, let σ be a positive constant and $f_{\min}$ the current lowest cost value. The hyper-box j is said to be potentially optimal if there exists some constant, the so-called Lipschitz constant, $K > 0$ such that

$$\begin{aligned} &f(x_j) - f(x_i) \le -K \cdot (d_i - d_j) \qquad \text{for any } i \\ &f(x_j) - K \cdot d_j \le f_{\min} - \sigma \cdot |f_{\min}| \end{aligned} \tag{11}$$

In order to avoid considering all the possible values of K, the potential hyper-boxes are those in the lower-right convex hull of a graphical alignment [28]. In the graph, each hyper-box is represented by a circle of which the horizontal coordinate is its size, and the vertical coordinate is the objective function value at its center point

Based on the DIRECT algorithm, we plan to optimize the multi-objective problem in the sense of Pareto optimality [16,31,32] since we assume no a priori preference among the conflicting objectives. The multi-objective DIRECT algorithm, abbreviated as MO-DIRECT, modify the selection strategy of the DIRECT algorithm while preserving its dividing strategy.

3.1. **The division strategy of MO-DIRECT.** Figure 3 demonstrates the first three iterations of an optimization problem with three design variables. At the start of iteration, the center points of the hyper-boxes are evaluated for objective values. DIRECT then selects one or more of the hyper-boxes for further search using a strategy to be described in Subsection 3.2. Finally, each selected hyper-box is trisected along one of its long sides. By trisection, the original centers remain at the center of resultant smaller hyper-boxes and only two new centers have to be evaluated for each division.

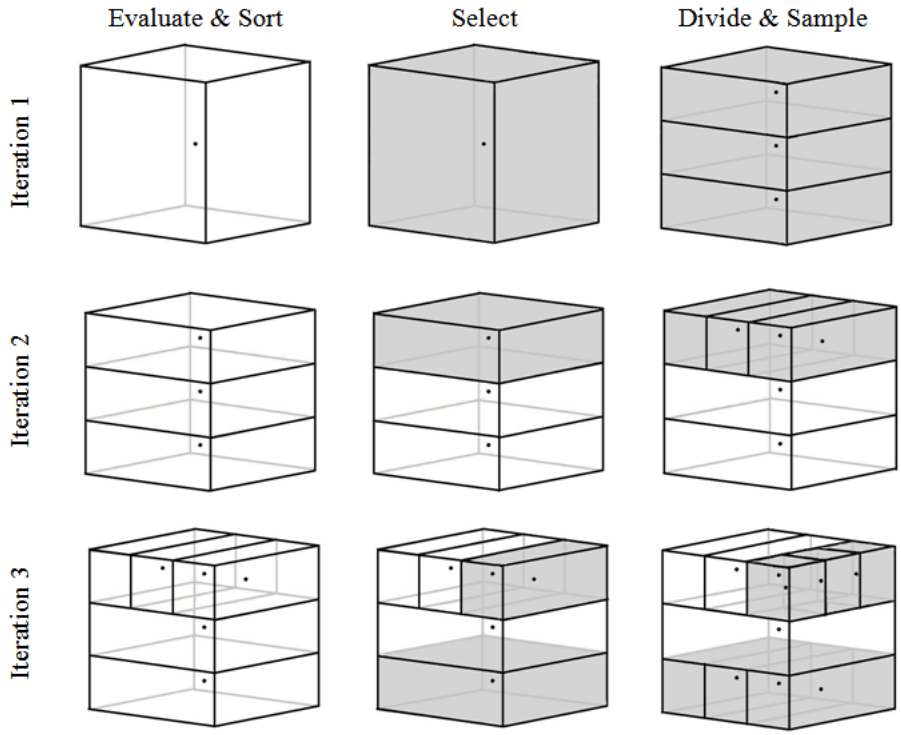

FIGURE 3. Illustration of the dividing strategy of the DIRECT algorithm in a three-dimensional search space

At the first iteration, there is only one hyper-box and the process of selection for trisection is trivial. It is then trisected into three hyper-rectangles, denoted as type-α. At the beginning of iteration 2, the selection process is nontrivial since there are 3 type-α hyper-boxes. In this example, we select just one hyper-box, which is then trisected into even smaller hyper-rectangles, denoted as type-β. At the start of iteration 3, there are 2 type-α hyper-boxes and 3 type-β hyper-boxes. For this demonstration, one of each type is selected and trisected, resulting in one type-α hyper-box, 5 type-β hyper-boxes, and 3 small hyper-cubes, denoted as type-γ.

If the design parameters are of finite resolution, the division procedure can be conveniently modified for integers by the introduction of the floor function, which is the greatest possible integer of the argument. For details regarding the floor function for center definition and trisecting manipulation, interested readers are referred to [28].

3.2. **The selection strategy of MO-DIRECT.** For the algorithm to be truly global, potential optimums should not be overlooked. On the other hand, local search near the current best solution is required for an efficient exploration. Thus, the main operation of the algorithm is to select all the potentially optimal hyper-boxes, and precede the partition strategy described in Subsection 3.1.

Selection strategy modified from the DIRECT algorithm is proposed for the multi-objective problem. We solve the problem in the sense of Pareto optimality, which is defined based on the concept of strict dominance and Pareto frontier [31,32], as described below.

Suppose x_1 and x_2 are vectors of the design variables, we have that x_1 strictly dominates q, denoted as $x_1 \succ x_2$, when every component of x_1 is not worse than x_2 and at least one

component is better. Furthermore, the set of vectors that are not strictly dominated by any other vectors is defined as the Pareto frontier.

In other words, a four-factor design vector $x^* \in \Omega$, with Ω being the domain of all candidate vectors, is in the Pareto frontier for two objectives, P_1 and P_2, if and only if there is no vector $x \in \Omega$ with the following characteristics

$$P_1(x) \geq P_1(x^*) \text{ and } P_2(x) \leq P_2(x^*) \tag{12a}$$

$$P_1(x) > P_1(x^*) \text{ or } P_2(x) < P_2(x^*). \tag{12b}$$

Since the solution x^* is not worse than x in all objectives (Equation (12a)) and x^* is strictly better than x in at least one objective (Equation (12b)), we have that x^* is not strictly dominated by x. The same concept can be applied with little modification to the optimization problems with more than two objectives.

Additionally, we may sort the population into ranks, such that members of the Pareto frontier are categorized as rank 1, and members of the newly emerged Pareto frontier when the original Pareto frontier is temporarily removed are categorized as rank 2, and so on for the subsequent members.

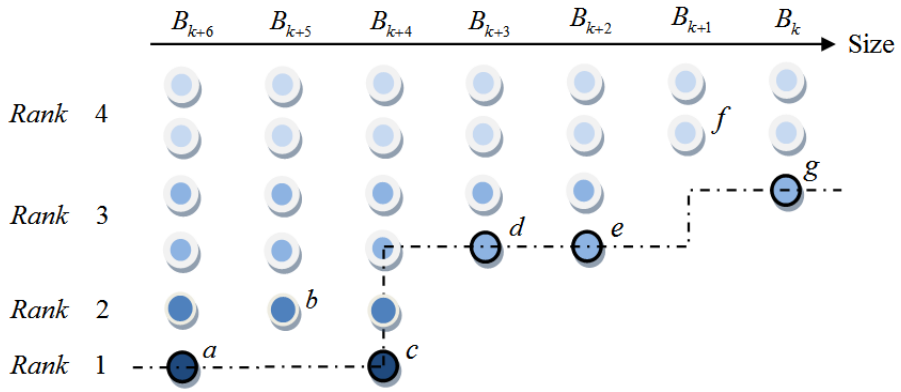

FIGURE 4. An illustrative example used to demonstrate how hyper-boxes are selected for dividing in the MO-DIRECT algorithm

With this ranking, we can now describe how hyper-boxes are selected for dividing by Figure 4. In the figure, the hyper-boxes are represented by circles which are gathered in size groups, denoted as B_k, $B_{k+1}, B_{k+2}, \ldots, B_{k+5}$ and B_{k+6}. Note that, in a size group, there might be more than one hyper-box with the same rank, and some ranks might be absent. For instance, there are two Rank 3 members in B_{k+6}, and no Rank 1 member in B_{k+5}. The selection strategy of MO-DIRECT can be briefly described as follows:

- Select the lowest rank member of a size group if there is no lower rank member in all of its right-hand side (larger) groups. When two or more hyper-boxes have the same lowest rank in a size group, a hyper-box is randomly selected for dividing.

According to the rule, hyper-boxes a, c, d, e and g are selected for division. Hyper-boxes b and f are skipped because there are lower rank members, c and g, in larger groups, B_{k+4} and B_k, respectively.

There are two differences between MO-DIRECT and the standard DIRECT algorithm in the selection strategy:

1. The MO-DIRECT is based on the Pareto ranking, while DIRECT is directly based on the objective value.

2. In MO-DIRECT, a hyper-box is selected even when there is a larger hyper-box with the same rank. In the standard DIRECT, if there is a larger hyper-box with the same objective value, the smaller one is ignored.

After several iterations, each size group will have a large number of candidate solutions sharing the same rank, especially in the smallest size group. Hence, the procedure can easily result in exhaustive search. To improve overall performance, we apply the crowding distance computation [33] to trim the hyper-boxes each iteration such that each size group has only a limited number, say 120 for example, of hyper-boxes with the same rank.

The basic procedure of MO-DIRECT is summarized by the following steps.

Step 1) Initialize the first hyper-box as the entire design space.
Step 2) Evaluate the center points of current hyper-boxes.
Step 3) Sort the hyper-boxes into Pareto ranks according to the results of Step 2.
Step 4) Trim the hyper-boxes such that each size group has only a limited number of hyper-boxes with the same rank.
Step 5) Select all of the potentially optimal hyper-boxes that satisfy the following two conditions:
  (1) It is of the lowest rank in its size group.
  (2) There is no lower rank member in all of its right-hand side (larger) groups.
Step 6) Trisect the selected hyper-boxes.
Step 7) Go back to Step 2 until the maximum number of function evaluations is reached or some termination criterion has been met.

3.3. **Artificial neural network as surrogate model.** In order to reduce the effort of numerical analysis in the optimization process, an artificial neural network (ANN) [34] is employed as surrogate model [18] for interpolation. Surrogate model accelerates the search for promising designs by replacing expensive design evaluations or simulations. They provide a global model of performance with respect to design variables, which can then be used in the optimization procedure efficiently.

Nine pilot simulations, with results listed in Table 1, were conducted for the training of neural networks that build the numerical relationships between the four processing parameters (n, Δr, d, and $\dot{m}$) and the two objective characteristics (effectiveness and pressure drop, P_1 and P_2).

We use a multilayered feed forward neural network [34] as the interpolation model. Without loss of generality, the artificial neural network (ANN) has two hidden layers. The number of the neurons in the two hidden layers was optimized by the standard DIRECT algorithm [35] to find an ANN with minimum prediction error. The Levenberg-Marquardt training algorithm was applied to train the network. Figure 5 shows the optimization history when a search space is defined as 40 by 40 for the number of neurons in the two hidden layers. In this figure, the temporarily best solutions for the iterations are connected together, showing the trace of search.

Within 58 steps, we have reached a global optimal structure design for the surrogate neural network, instead of 1,600 trials in an exhaustive search. The optimized 4-5-2-2 network was then employed in the following procedure.

3.4. **Overall optimization method – MO-DIRECT and ANN.** The optimization procedure combines the surrogate model and the MO-DIRECT algorithm to find the optimal design in the sense of Pareto optimality.

As shown in Figure 6, the design procedure begins with the preparation of pilot simulation data for the surrogate model using computational fluid dynamics (CFD) described in Section 2. These data are not only used for the training of ANN, but also for the

design of number of nodes in the hidden layers, since the architecture of an ANN plays an important role in its approximation and interpolation. The ANN architecture design is based on the integer DIRECT algorithm, as described in Subsection 3.3. Once trained, the ANN is ready for supplying the corresponding performance values, P_1 and P_2, for

TABLE 1. Pilot simulation data showing the numerical relationships between the 4 design parameters (n, Δr, d, and $\dot{m}$) and the corresponding two design goals (effectiveness and pressure drop, P_1 and P_2)

Number of turns n	**Channel width (mm)** Δr	**Plate thickness (mm)** d	**Mass flow rate (kg/s)** $\dot{m}$	**Effectiveness** P_1	**Pressure loss** P_2
6	5.8	1.4	0.154	0.599064	0.12632
7	5.8	1.4	0.154	0.672532	0.165355
8	5.8	1.4	0.154	0.736521	0.20978
6	4.8	1.4	0.154	0.638066	0.202734
6	6.8	1.4	0.154	0.573862	0.085878
6	5.8	1.0	0.154	0.590622	0.122071
6	5.8	2.0	0.154	0.611164	0.132729
6	5.8	1.4	0.125	0.601523	0.086416
6	5.8	1.4	0.175	0.5998	0.159784

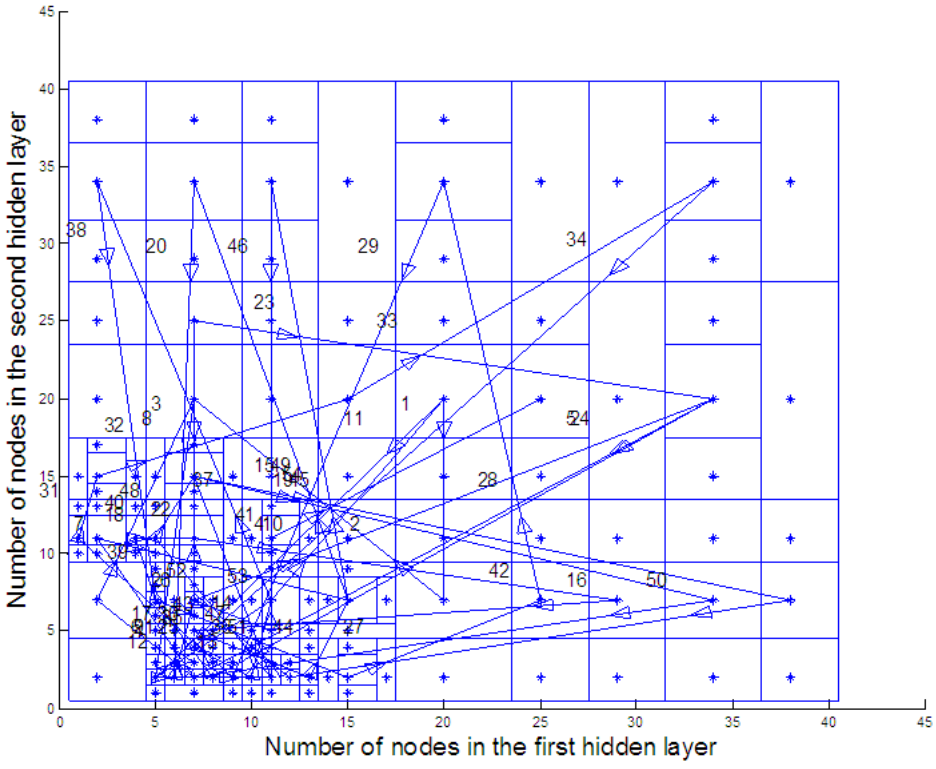

FIGURE 5. Searching history in optimizing the size of the hidden layers of the surrogate ANN

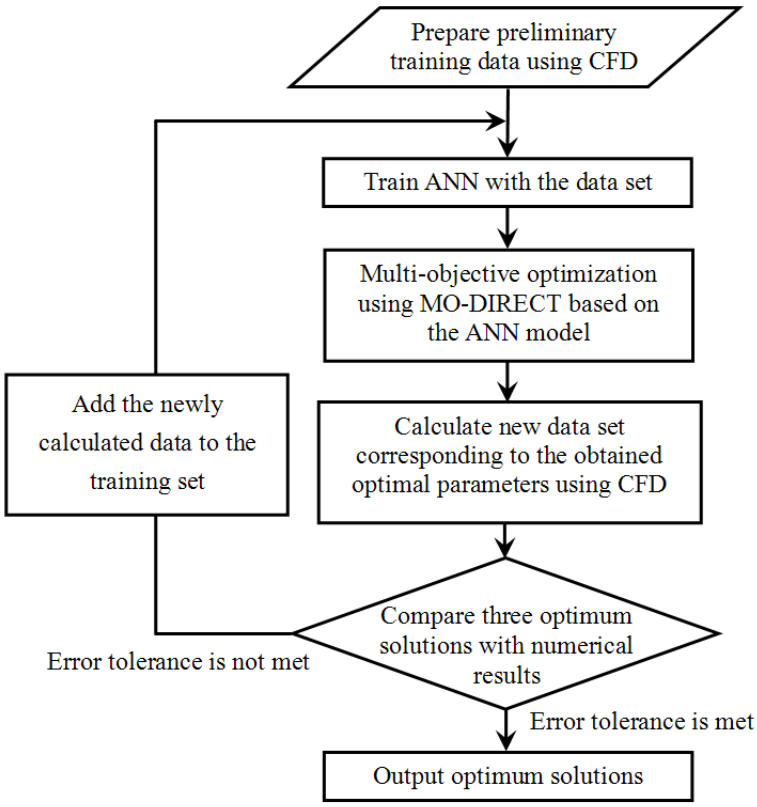

FIGURE 6. Flow chart of the design procedure showing the interaction between the MO-DIRECT algorithm and the ANN surrogate model

each combination of design parameters without the computationally intensive numerical simulations.

Optimization of the recuperator is then directed by the MO-DIRECT algorithm to find the best combination of design parameters (n, Δr, d, and $\dot{m}$) in the Pareto front. Since there are infinitive solutions in the Pareto front, theoretically, we select two extremes and one min-max solution as representatives. Correctness of these three solutions is verified by the deviation between the performances (P_1 and P_2) obtained by the surrogate model and those calculated by numerical simulations.

If the deviation, or the prediction error, is larger than a predefined value, the newly calculated numerical data should be included in the training data set, and we re-train the ANN to fit the augmented data set. After that, the MO-DIRECT algorithm is used in the next iteration to find the updated Pareto front. These procedures are repeated until the prediction error is small enough.

4. **Effectiveness of the Proposed Scheme.** As shown in Table 2, mere four iterations are required to find an optimal solution set with prediction error lower than 4%. The prediction errors are further plotted in Figure 7, showing the convergence trend. Note that the prediction error of the first cost value (P_1) is always higher than that of the second cost value (P_2), but both converge to a very small value at the end of the fifth iteration.

Figure 8 shows the Pareto front obtained at the end of the iterations, with an optimum min-max solution of $n = 8$, $\Delta r = 5.4$, $d = 2.0$, and $\dot{m} = 0.125$. It is worth to mention that only 2,313 cost function evaluations (derived from the ANN) are required to obtain the representative Pareto front solutions. This is much less than the exhaustive search

TABLE 2. Record of five optimization iterations. In each iteration, 3 prediction sets of design goals (P_1 and P_2) from the Pareto front are obtained using the ANN model. The design goals are compared with the numerical simulation results.

Pareto front solutions	n	Δr	d	$\dot{m}$	*From ANN model*		*From numerical simulation*	
					P_1	P_2	P_1	P_2
First Run								
Max P_1	8	4.9	1.9	0.175	0.7567	0.215	0.80565465	0.452689
Min P_2	6	6.6	1	0.125	0.5969	0.0474	0.57102686	0.065755
Min-max	7	5.9	1.4	0.125	0.6586	0.151	0.66669985	0.108078
Second Run								
Max P_1	8	6.8	2	0.175	0.9907	0.5728	0.71786351	0.200607
Min P_2	6	6	1	0.125	0.5815	0.0511	0.58527661	0.082323
Min-max	8	6.2	1.9	0.156	0.8075	0.2846	0.73268428	0.190305
Third Run								
Max P_1	8	5.9	1	0.175	0.8794	0.8185	0.72649195	0.261244
Min P_2	7	6.8	1.9	0.135	0.6106	0.0497	0.65519866	0.091948
Min-max	8	4.8	1.9	0.164	0.7792	0.3414	0.8077586	0.400965
Fourth Run								
Max P_1	7	4.8	2	0.127	0.8263	0.6054	0.71825323	0.196222
Min P_2	7	6.5	1.2	0.125	0.661	0.0459	0.6472422	0.089818
Min-max	8	5.6	1.1	0.125	0.7637	0.2577	0.7259323	0.159855
Fifth Run								
Max P_1	8	4.8	2	0.167	0.8123	0.4225	0.81369663	0.419631
Min P_2	6	6.8	1.5	0.125	0.5778	0.0628	0.57838252	0.063465
Min-max	8	5.4	2	0.125	0.7416	0.1731	0.75410927	0.179565

which requires 35,343 evaluations. (Based on the fact that n has 3 different values: 6, 7, 8, Δr has 21 alternatives: 4.8 to 6.8 with resolution 0.1, d has 11 alternatives: 1.0 to 2.0 with resolution 0.1, and $\dot{m}$ has 51 alternatives: 0.125 to 0.175 with resolution 0.01; $3 \times 21 \times 11 \times 51 = 35,343$.)

As the ANN represents the relationship between the design parameters and the design goals, it is ready to be investigated for trends. Figure 9 and Figure 10 show the variation of effectiveness and the pressure loss with respect to the flow rate and plate thickness. It is clear that both design goals increase with the increase of these two design parameters, thus a trade-off is required for this two-objective problem. Note that, as there are four design parameters, two of them (the number of turns and channel width) must be fixed to plot these three dimensional figures.

Furthermore, there are nine primary simulations to collect data to train the ANN, and five iterations of MO-DIRECT, each requires three simulations to verify correctness of the surrogate model, totally only 24 numerical simulations are required to reach the two-objective global optimization design. Considering that each numerical simulation takes more than 15 minutes when a Intel Core i7-2630QM 2.0 GHz CPU equipped with 4 GB main memory are used, the proposed design procedure is efficient enough for practical design applications.

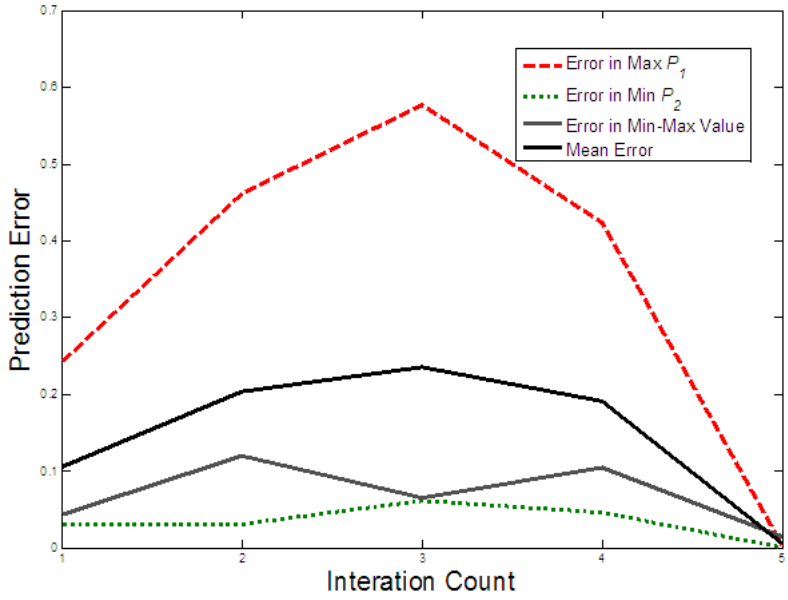

FIGURE 7. Convergence history of the prediction errors of the ANN surrogate model

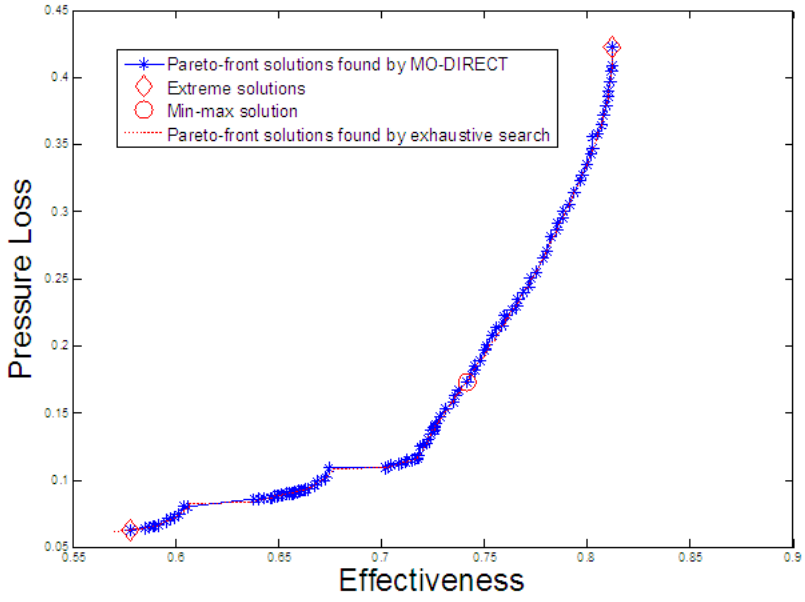

FIGURE 8. The Pareto front obtained by the MO-DIRECT optimization algorithm

5. **Conclusion.** An effective multi-objective design procedure is proposed for the design of Swiss-roll recuperator that is used as a heat exchanger to recover the exhaust heat of a micro gas turbine.

Preliminary theoretical analysis of the recupeator shows that the complex interconnections between these design parameters make it difficult to analyze the process and select adequate parameter combination to build a recuperator with the highest effectiveness and lowest pressure drop. We take the number of turns, channel width, plate thickness, and

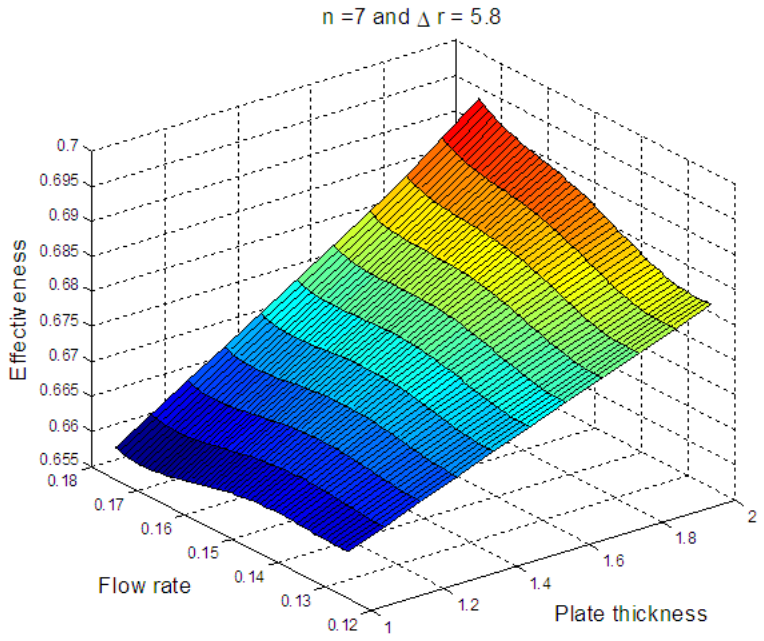

FIGURE 9. The influence of flow rate and plate thickness on the effectiveness of the Swiss-roll recuperator

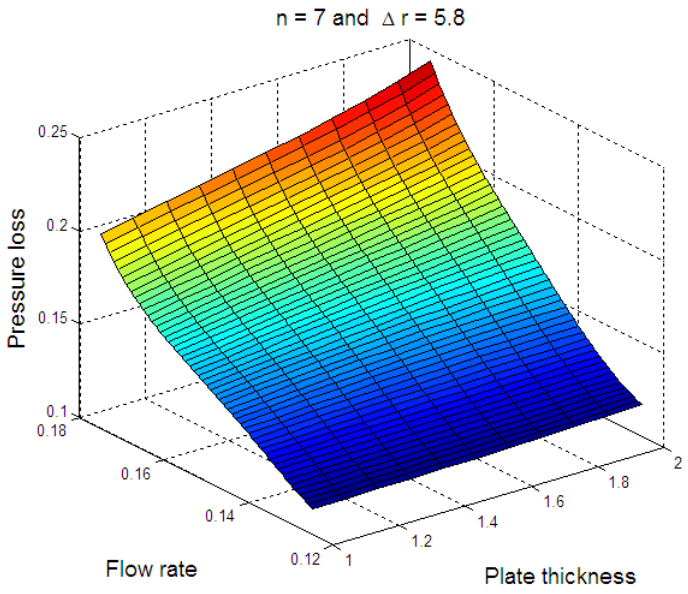

FIGURE 10. The influence of flow rate and plate thickness on the pressure loss of the Swiss-roll recuperator

mass flow rate, totally four design parameters, to be optimized for these two objectives in the sense of Pareto optimality.

In order to reduce the number of numerical analysis in the optimization procedure, a two-layered feed-forward neural network is employed as surrogate model, and a multi-objective DIRECT algorithm, named as MO-DIRECT, is developed. The structure of the neural network was optimized by the normal DIRECT algorithm, resulting in a 4-5-2-2 network.

After merely 5 iterations, with 3 representative parameter sets selected from the Pareto front for correctness test of the surrogate model in each iteration, we were able to find a min-max solution with prediction error lower than 4%. Also, only 24 numerical simulations are required to achieve the results, and only 2,313 steps were conducted in the MO-DIRECT search, rather than 35,343 required for an exhaustive search.

Acknowledgment. The authors are enormously grateful for the support from the National Science Council, Taiwan, and the Technology Development Program for Academia (TDPA) of the Ministry of Economic Affairs under contract number NSC-99-2221-E-182-012, NSC100-2221-E-182-008, NSC100-2221-E-182-053-MY2, and 99-EC-17-A-19-S1-035. The authors also gratefully acknowledge the helpful comments and suggestions of the reviewers, which have improved the presentation.

REFERENCES

[1] A. D. Little, Opportunities for micropower and fuel cell/gas turbine hybrid systems in industrial applications, *DOE Report*, Subcontract No. 85X-TA009V, 2000.

[2] C. F. McDonald and C. Rodgers, The ubiquitous personal turbine – A power vision for the 21st century, *J. of Engineering for Gas Turbines and Power*, vol.124, no.4, pp.835-844, 2002.

[3] C. F. McDonald, Heat recovery exchanger technology for very small gas turbines, *Int. J. of Turbo and Jet Engines*, vol.13, no.4, pp.239-261, 1996.

[4] H. Y. Shih, D. Wang and C. R. Kuo, Feasibility study of an innovative micro gas turbine with a Swiss-roll recuperator, *Proc. of ASME Turbo Expo*, vol.5, part A, pp.459-466, 2006.

[5] H. Y. Shih and Y. C. Huang, Thermal design and model analysis of the Swiss-roll recuperator for an innovative micro gas turbine, *Applied Thermal Engineering*, vol.29, no.8-9, pp.1493-1499, 2009.

[6] B. J. Tsai and Y. L. Wang, A novel Swiss-roll recuperator for the microturbine engine, *Applied Thermal Engineering*, vol.29, no.2-3, pp.216-223, 2009.

[7] S. A. Lloyd and F. J. Weinberg, A burner for mixtures of very low heat content, *Nature*, vol.251, pp.47-49, 1974.

[8] S. A. Lloyd and F. J. Weinberg, Limits to energy release and utilization from chemical fuels, *Nature*, vol.257, pp.367-370, 1975.

[9] A. C. Fernandez-Pello, Micropower generation using combustion: Issues and approaches, *Proc. of the Combustion Institute*, vol.29, no.1, pp.883-898, 2002.

[10] N. II Kim, S. Kato, T. Kataoka, T. Yokomori, S. Maruyama, T. Fujimori and K. Maruta, Flame stabilization and emission of small Swiss-roll combustors as heaters, *Combustion and Flame*, vol.141, no.3, pp.229-240, 2005.

[11] J. Ahn, C. Eastwood, L. Sitzki, P. D. Ronney, A. K. Agrawal, C. Cadou, D. C. Kyritsis and D. Vlachos, Gas-phase and catalytic combustion in heat-recirculating burners, *Proc. of the Combustion Institute*, vol.30, no.2, pp.2463-2472, 2005.

[12] N. II Kim, S. Aizumi, T. Yokomori, S. Kato, T. Fujimori and K. Maruta, Development and scale effects of small Swiss-roll combustor, *Proc. of the Combustion Institute*, vol.31, no.2, pp.3243-3250, 2007.

[13] C. H. Kuo and P. D. Ronney, Numerical modeling of non-adiabatic heat recirculating combustors, *Proc. of the Combustion Institute*, vol.31, no.2, pp.3277-3284, 2007.

[14] Q. Li, G. Flamant, X. Yuan, P. Neveu and L. Luo, Compact heat exchangers: A review and future applications for a new generation of high temperature solar receivers, *Renewable and Sustainable Energy Reviews*, vol.15, no.9, pp.4855-4875, 2011.

[15] H. Xu, Y. Zou and S. Xu, Non-fragile robust H_∞ control for uncertain 2-D delayed systems described by the general model, *International Journal of Innovative Computing, Information and Control*, vol.5, no.10(A), pp.3179-3187, 2009.

[16] N. Wang and Y. Chang, Application of the genetic algorithm to the multi-objective optimization of air bearings, *Tribology Letters*, vol.17, no.2, pp.119-128, 2004.

[17] A. Fekih, Neural networks based system identification techniques for model based fault detection of nonlinear systems, *International Journal of Innovative Computing, Information and Control*, vol.3, no.5, pp.1073-1085, 2007.

[18] A. Forrester, A. Sobester and A. Keane, *Engineering Design via Surrogate Modelling: A Practical Guide*, John Wiley, New York, 2008.

[19] D. E. Finkel, *DIRECT Optimization Algorithm User Guide*, Center for Research in Scientific Computation, North Carolina State University, 2003.
[20] J. Li, D. Wan, Z. Chi and X. Hu, An efficient fine-grained parallel particle swarm optimization method based on GPU-acceleration, *International Journal of Innovative Computing, Information and Control*, vol.3, no.6(B), pp.1707-1714, 2007.
[21] H. Xing, D. Li and X. Zhong, Sliding mode control for a class of parabolic uncertain distributed parameter systems with time-varying delays, *International Journal of Innovative Computing, Information and Control*, vol.5, no.9, pp.2689-2702, 2009.
[22] L. Trom, Use spiral plate exchangers for various applications, *Hydrocarbon Processing*, vol.74, no.5, pp.73-80, 1995.
[23] H. Martine, *Heat Exchangers*, Hemisphere Publishing Co., London, 1992.
[24] T. Bes, Thermal design of spiral heat exchangers, *Int. J. Heat Exchangers*, vol.2, pp.59-96, 2001.
[25] STAR-CD, *Computational Fluid Dynamics Software*, CD Adapco Group.
[26] S. V. Patankar, *Numerical Heat Transfer and Fluid Flow*, 1980.
[27] D. R. Jones, C. D. Perttunen and B. E. Stuckman, Lipschitzian optimization without Lipschitz constant, *Journal of Optimization Theory and Applications*, vol.79, no.1, pp.157-181, 1993.
[28] C. A. Floudas and P. M. Pardalos, *Encyclopedia of Optimization*, Kluwer Academic Publishers, London, 2001.
[29] H. Zhu and D. B. Bogy, DIRECT algorithm and its application to slider air-bearing surface optimization, *IEEE Trans. on Magnetics*, vol.38, no.5, pp.2168-2170, 2002.
[30] H. Zhu and D. B. Bogy, Hard disc drive air bearing design: Modified DIRECT algorithm and its application to slider air bearing surface optimization, *Tribology International*, vol.37, no.2, pp.193-201, 2004.
[31] C. A. C. Coello, D. A. Van Veldhuizen and G. B. Lamont, *Evolutionary Algorithms for Solving Multi-Objective Problems*, 2nd Edtion, Springer, New York, 2007.
[32] J. Knowles, D. Corne and K. Deb, *Multiobjective Problem Solving from Nature: From Concepts to Applications*, Springer-Verlag, Berlin, 2008.
[33] M. Kaya, MOGAMOD: Multi-objective genetic algorithm for motif discovery, *Expert Systems with Applications*, vol.36, no.2, pp.1039-1047, 2009.
[34] F. M. Ham and I. Kostanic, *Principles of Neurocomputing for Science and Engineering*, McGraw-Hill, 2001.
[35] J. M. Gablonsky, An implementation of the DIRECT algorithm, *Technical Report CRSC-TR98-29*, Center for Research in Scientific Computation, North Carolina State University, 1998.